J. Water Environ. Nanotechnol., 6(2): 92-108 Spring 2021

ORIGINAL RESEARCH PAPER

Sol-Gel to Prepare Nickel Doped TiO_2 Nanoparticles for Photocatalytic Treatment of E 131 VF Food Dye Wastewater

Malak Barakat[1], Rassil Khoder[1], Fatima Kassir[1], Zeinab Harajli[1], Mouhiaddine Mohamed El Jamal[1*], Azadeh Ebrahimian Pirbazari[2*]

[1] Inorganic and Organometallic Coordination Chemistry Laboratory (LCIO), Faculty of Sciences (I), Lebanese University, Rafic Hariri Campus, El Hadath, Lebanon
[2] Fouman Faculty of Engineering, College of Engineering, University of Tehran

Received: 2021-01-16 Accepted: 2021-02-19 Published: 2021-05-01

ABSTRACT

The sol-gel method was applied for the synthesis of TiO_2 nanoparticles in the existence of different volumes of ethanol (10–50 mL) with the purpose to find optimized synthesis conditions. Also, nickel-doped TiO_2 nanoparticles (Ni/TiO_2 molar ratio: 0.1-1.0%) were prepared by a similar technique but in the existence of 10 mL ethanol and heated at different temperatures (300 °C –600 °C). XRD, SEM/EDX, UV-Vis DRS, FTIR, and Raman spectroscopy were applied to identify the structural and morphological characteristics of the as-synthesized samples. XR diffraction results verified that TiO_2 samples prepared with various volumes of ethanol (10–50 mL) consist of anatase and brookite phases up to 500 °C and rutile phase at 600 °C. The intensity of brookite diffraction decreased with the increase of calcination temperatures. Also, the low ethanol volume was favored for the formation of the rutile phase at 600 °C. The addition of Ni(II) during the preparation of TiO_2 nanoparticles prevented the formation of the rutile phase. The undoped samples were synthesized with 10 and 20 mL ethanol and treated at 500 °C displayed the best catalytic performance for the photocatalytic treatment of E 131 VF dye solution (rate constant: 0.051 and 0.061 (a.u) respectively). Ni-doped TiO_2 samples displayed lower photoactivity and rate constant.

Keywords: *Sol-gel, Ni/TiO_2, Ethanol, Food dye E 131 VF, Kinetic study.*

How to cite this article
Barakat M., Khoder R., Kassir F., Harajli Z., El Jamal MM, Ebrahimian Pirbazari A. Sol-Gel to Prepare Nickel Doped TiO_2 Nanoparticles for Photocatalytic Treatment of E 131 VF Food Dye Wastewater. J. Water Environ. Nanotechnol., 2021; 6(2): 92-108.
DOI: 10.22090/jwent.2021.02.001

INTRODUCTION

Today, the development of industries and unexpected increase in population has caused the whole world to face environmental problems. The discharge of large amounts of wastewater into water resources and the lack of safe water have caused serious concerns for communities due to the dependence of the well-being of humans and ecosystems on the availability and quality of water [1]. One of the effective methods to protect the environment is the removal of organic pollutants from the effluent [2]. Food dyes such as (E 131 VF (blue), E 102 (yellow), E 123 (red)) are the most important kind of organic pollutants and dangerous food additives. In order to improve taste, attract consumers, and even adapt to the food culture; food dyes have become one of the essential links in modern food processing [3]. Some studies show that artificial food dyes affect children's intelligence, cause hyperactivity, and allergy when children consumed ≥ 50mg [3]. Many dyes persist

* Corresponding Author Email: *aebrahimian@ut.ac.ir*
mjamal@ul.edu.lb

in the environment and when they discharge in water bodies, they commonly decrease sunlight transmission and affect the life of living beings. So, various techniques were developed for the treatment of industrial wastewater before its discharge into the environment [4]. Several methods were employed for wastewater treatment such as electrochemical oxidation [5], adsorption [6], chemical oxidation [7], biological treatment [8], etc. However, they are either slow or non-destructive for some organic pollutants. In the past two decades, heterogeneous photocatalytic oxidation has attracted enormous attention. Complete mineralization of various organic compounds into harmless products is achieved via heterogeneous photocatalytic oxidation [9]. It is a process, in which the rate of photoreaction is accelerated in the presence of a semiconductor catalyst. Several semiconductors [10], ZnO [11], Fe_2O_3 [12], and ZnS [13] can act as photocatalysts, but TiO_2 frequently has been most applied, owing to its properties (high photochemical stability, inexpensive, etc) [14]. TiO_2 is widely used in a variety of applications in the environmental and energy fields' conservation, water purification, and cancer treatment [14]. TiO_2 includes three different crystalline phases: anatase, rutile, and brookite [15]. The rutile phase of TiO_2 is the most thermodynamically stable, while anatase and brookite phases are metastable and simply changed to the rutile phase through calcination [3, 14]. The physical characteristics of the three forms of TiO_2 are very dissimilar and depending on the preparation conditions [16, 17]. The anatase phase is mostly used as a photocatalyst, due to its high photocatalytic activity, whereas the rutile phase has low activity [17]. Anatase with higher crystallinity is favored for photocatalysis reactions. There are no many reports about using the brookite phase of TiO_2 in the photocatalytic degradation process due to the difficulties to obtain it as a pure phase [17]. In the heterogeneous photocatalysis process, radiation with energy more than the bandgap energy of semiconductor could initiate charge carriers generation (electron and hole), and an electron transfers from the valance band (VB) to the conduction band (CB) of the semiconductor. It produces a positive hole (h^+) at the valance band and an electron (e^-) in the conduction band [15]. The electron could reduce an acceptor, while the positive hole could oxidize a donor. The free electrons react with the adsorbed oxygen to form superoxide radical anions ($O_2^{\bullet}$). In the presence of adsorbed protons (H^+), the superoxide anion could produce hydroperoxide radical ($HO_2^{\bullet}$) and later on hydrogen peroxide (H_2O_2), which could decompose under radiation on the catalyst surface, or react with $O_2^{\bullet}$ to form hydroxyl radical ($OH^{\bullet}$). Also, positive holes (h^+) could react with water (H_2O) to form hydroxyl radicals ($OH^{\bullet}$) or oxidize directly the organic compounds. Thus, the generated radicles ($OH^{\bullet}$, $O_2^{\bullet-}$) are very reactive and could oxidize the compounds and completely mineralize them [18]. However, the fast recombination of the electron-hole pairs retard active species generation and lowering the photoactivity of the catalyst [19]. Various synthesis methods such as sol-gel [20], hydrothermal [21], solvothermal [22], electrochemical [23], microwave method [24], and microwave-assisted solvothermal [25] have been used to synthesis TiO_2. The Sol-gel route is the easiest and inexpensive method and has been widely employed for predation of titanium dioxide particles. In the sol-gel synthesis method, when an organometallic precursor is added to water, two reactions of hydrolysis and condensation are performed simultaneously. Both of these reactions are sensitive to several parameters such as precursor concentration, hydrolysis temperature, stirring conditions, and pH [26]. Most photocatalysts, including titanium dioxide, have limitations such as low surface area, low adsorption capacity, and high recombination rate [27]. Researches have shown that the heterogeneous photocatalytic degradation is based on the generation of charge carriers during irradiation and recombination should be largely avoided [28]. Thus, numerous researches have been performed to boost the efficiency of TiO_2 by declining the charge carrier recombination and the modification of its electrical/optical properties [28]. In this regard, various elements such as noble metals and transition metals as well as nonmetals and metalloids are doped in the photocatalyst to modify its properties [28]. Recent studies show that doping TiO_2 with certain metal ions such as Cu^{2+} [18] and Co^{2+} [29] have reduced its photocatalytic activity under UV irradiation. Nickel doping in titanium dioxide has been performed to improve its photocatalytic activity and to extend its absorption spectrum to the visible region[30]. In another study, the performance of nickel doped titanium dioxide samples was investigated for photodegradation of methylene blue under visible light [31]. The results showed that nickel doping caused anatase phase stability,

presented better structural, morphological and dielectric property and also reduced the band gap energy of TiO_2[31]. Several parameters such as pH, temperature of calcination, nature of the organic solvent affect TiO_2 properties such as photoactivity [18], morphology [32], crystalline phase [23] and electrical properties [33]. These parameters have significantly influenced the TiO_2 degradation performance. A recent report on the synthesis of titanium dioxide nanoparticles using the sol-gel method in the presence of different volumes of acetic acid has shown that the transfer of anatase phase to rutile phase depends on the volume of acetic acid and the calcination temperature [18]. Due to the above-mentioned reasons, in this study we tried to synthesize TiO_2 nanoparticles using sol-gel method in the presence of ethanol to investigate the effect of different volumes of it on the structural properties of titanium dioxide nanoparticles.

In this study, in order to find the best conditions for the synthesis, the titanium precursor (TTIP) amount was kept constant and the as-synthesized catalysts were calcined at different temperatures (300°C–600 °C). Nickel-doped titanium dioxide samples (Ni/TiO_2 molar ratio: 0.1–1.0%) were prepared under optimal conditions and calcined at different temperatures. Finally, the efficiency of the synthesized samples was investigated for the photocatalytic treatment of E 131 VF food dye wastewater. This study could highlight how the earlier synthesis conditions such as the volume of ethanol, water amount, calcination temperature, and doping metal can influence the structural properties of the final products.

MATERIALS AND METHODS

Synthesis of Ni-doped TiO_2

Titanium (IV) isopropoxide (TTIP, 98%) and ethanol (95%) were obtained from Acros Organics and Sigma Aldrich, Germany respectively. E 131 VF dye (a food colorant) as an organic pollutant model was bought from Sigma Aldrich ($C_{27}H_{31}N_2O_6S_2$-Na, purity: 50%, MW: 565.67 g) and nickel salt ($NiCl_2.6H_2O$ (99%)) was obtained from BDH (GPR). TiO_2 nanoparticles were obtained by the sol-gel method in the presence of different volumes of ethanol and the preparation details can be found in ref [18]. The obtained catalysts were calcined at 300, 400, 500, and 600 °C for 4h (in an air atmosphere) to induce the crystallization and investigate the stability of the TiO_2 phase as a function of temperature. The prepared TiO_2 was named "x Eth TiO_2 T"; which x stands for the ethanol volume (mL) and T is the temperature (°C). The best photocatalytic performance was achieved for the samples that were prepared with 10 and 20 mL ethanol and treated at 500 °C. We prepared nickel-doped samples by a similar method with 10 mL ethanol and treated them at different temperatures for 4h. These samples were labeled "x% Ni T"; which x stands for the Ni/TiO_2 molar ratio (0.1–1.0%) and T is the temperature.

Photocatalytic Degradation tests

To perform the photocatalytic degradation test, a suspension containing 100 mL of E 131 VF dye solution (Conc: 20 mg/L) and 0.08 g of catalyst was first stirred in the dark for 15 minutes to achieve adsorption and desorption equilibrium. The suspension was irradiated with three UVC lamps (λ_{max} = 256 nm) placed 10 cm above the glass bowl (Luzchem LZC-4V, Canada). Degradation tests were also performed in the presence of different lamps to examine the effect of different wavelengths on the photoactivity of the samples. A fan was used during the irradiation period to eliminate the heat produced by the lamps and keep the reactor temperature constant at 28 °C. The photocatalytic degradation reaction was followed by a spectrophotometer at λ_{max}= 640 nm of E 131 VF dye.

Characterization

In order to evaluate the crystallinity of the synthesized samples and calculate the percentage of rutile phase, X-ray diffraction patterns were obtained using D8 Focus, Bruker, X-ray diffractometer in the range of 2θ = 10–80° equipped by a copper cathode (K_α radiation, λ= 0.1541nm) at the voltage of 50 kV. The percentage of rutile phase in the as-prepared catalysts was determined by equation (1):

$$\text{Rutile (weight \%)} = \frac{1}{\left(1+0.884\times\frac{\mathbf{I_A}}{\mathbf{I_R}}\right)}\times 100 \qquad (1)$$

Where I_A and I_R are the diffraction intensity of anatase and rutile phases, respectively [34].

The mean crystal dimension of TiO_2 was obtained by the Scherrer equation (Eq. 2):

$$D = K\lambda / (\beta \cos\theta) \qquad (2)$$

In this equation, θ is the angle of diffraction, K

is a constant (0.89), β refers to the diffraction full width at half maximum (FWHM) in radian for diffraction at 2θ = 25.3°, D shows mean dimension and λ represents the X-ray wavelength (0.1541 nm).

The lattice parameters of the samples obtained according to Eq. 3:

$$\frac{1}{d^2} = \frac{(h^2 + k^2)}{a^2} + \frac{l^2}{c^2} \quad (3)$$

a, b and c are the lattice parameters (for tetragonal lattice a = b ≠ c). The lattice parameters (a and c) were determined using the d values of the planes (200) and (101) (anatase phase) respectively [29]. Also, we obtained the unit cell volume by the following equation (4):

$$V = a^2 c \quad (4)$$

The functional groups on the catalysts were recognized using FTIR spectrometer (Jasco FT/IR-6300 spectrometer in the wavenumber range of 400 to 4000 cm^{-1}) and Raman spectrometer (Horiba Scientific, operating with green Laser at 532 nm). Scanning electron microscopy (SEM) micrographs and EDX spectra of the catalysts were prepared by Tescan MIRA 3 LMU combined with Inca X-max 20 from Oxford instrument (working distance: 15 mm, voltage 20 kV). Also, UV-Vis diffuse reflectance spectra were recorded using Jasco V-570 spectrophotometer in order to calculate the bandgap energy of the photocatalysts.

RESULTS AND DISCUSSION

Characterization of the catalysts

X-ray diffraction analysis

We detected four primary diffractions of anatase phase at 2θ = 25.3° (100%), 38° (20%), 48.2° (28%) and 62.5° (10%) (Fig.1a) in the XRD patterns of TiO_2 samples that were synthesized in the existence of 10 mL ethanol and calcined at various temperatures (120–600 °C)[18]. The diffractions at 2θ = 27.36° (100%), 36.0° (45%), 54.0° (53%), and 69.0° (8%) correspond to pure rutile phase [35]. The diffraction at 2θ =30.8° belongs to the brookite phase [36]. There is a mixture of anatase and brookite phases at temperatures up to 500

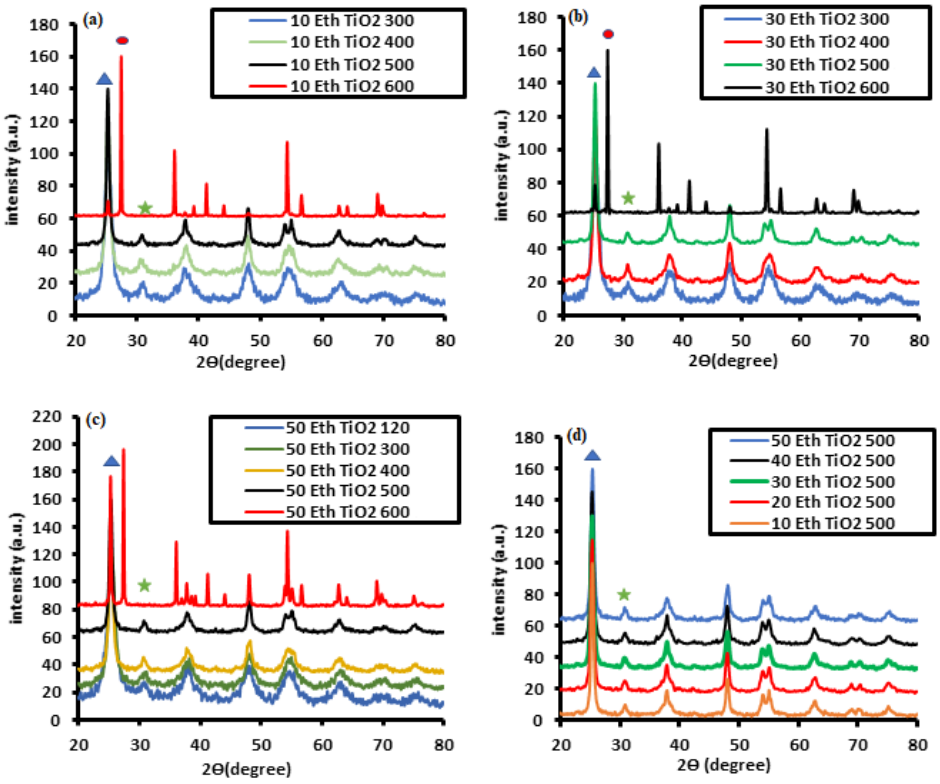

Fig. 1. XRD patterns of TiO_2 prepared with different volumes of ethanol and calcined at different temperatures: (a) 10 mL Eth, (b) 30 mL Eth, (c) 50 mL Eth, (d) all Eth volumes at 500 °C
(▲Anatase phase, ● Rutile Phase, ★brookite phase)

Table 1. Relative intensity of brookite prepared by different volumes of ethanol and calcined at different temperatures.

	Temperature	300 °C	400 °C	500 °C	600 °C
Intensity of brookite	10 mL Eth	19	13	10	-
	30 mL Eth	21	14	10	-
	50 mL Eth	15	9	5	-

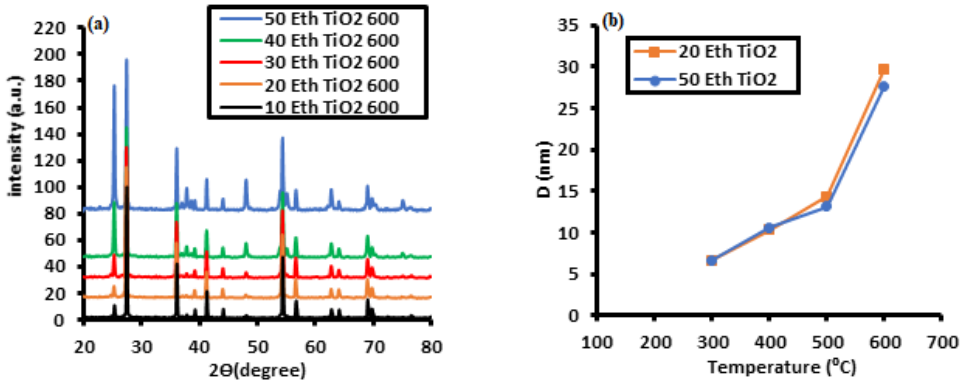

Fig. 2. a) XRD patterns of TiO_2 powder prepared with different volumes of ethanol and calcined at 600°C and b) average crystal size of TiO_2 as a function of calcination temperature

Table 2. Relative intensity of some characteristic peaks of the prepared samples at 600 °C

Sample	2θ =27.36° (I_R)	2θ =25.3° (I_A)	% I_R/I_A
10 mL Eth	100	10.78	91.29
20 mL Eth	100	10.19	91.73
30 mL Eth	100	18.80	85.74
40 mL Eth	100	43.49	72.22
50 mL Eth	100	96.58	57.64

°C. The relative intensity of brookite diffraction decreases from 19 (a.u.) to 10 (a.u.) with increasing the calcination temperature from 300 °C to 500 °C. However, at 600 °C there is no more brookite phase (Table 1) and both the anatase and rutile phases are present.

Similar observation reported by Sapcharoenkun and *et al* [37], increasing the calcination temperature increased the aggregation of crystallites leading to larger crystallite size since the anatase and brookite phases were completely transformed to rutile phase. This confirms that the crystallite size of TiO_2 powder was increased at a high temperature due to the larger crystallite size of the rutile phase. This could be attributed to the thermally promoted crystallite growth. Also, the transformation rate among different TiO_2 phases depends on the particle size and the aggregation state. For instance, it was reported that the transformation rate of anatase to rutile is increased dramatically when the reacting anatase is very finely crystalline and aggregated due to increased contact sites between the nanoparticles which are suggested to be the potential nucleation sites [38].

The intensity of anatase and brookite diffractions approximately remained constant in the XRD patterns of TiO_2 samples that synthesized in the presence of different volumes of ethanol (10-50 mL) and were calcined at 500 °C (Fig. 1d).

The XR diffraction patterns of TiO_2 prepared by different volumes of ethanol (10-50 mL) and calcined at 600 °C showed that the increase in ethanol volume was associated with the increase in anatase intensity (Fig. 2, Table 2). In another word, using large volumes of ethanol favored the formation of the anatase phase. At high concentration levels of ethanol, ethoxide adsorbs on Ti^{4+} cations prevent the corner-sharing and facilitates edge-sharing to promote anatase [39].

In our work, the use of ethanol resulted in

Table 3. Lattice parameters of TiO_2 that calcined at different temperatures (for rutile phase *62.06).

Temperature	a(Å)	b(Å)	c(Å)	V (Å^3)
10 Eth TiO_2 300	3.798	3.798	9.25	133.42
10 Eth TiO_2 400	3.798	3.798	9.18	133.42
10 Eth TiO_2 500	3.786	3.786	9.45	135.45
10 Eth TiO_2 600	3.785	3.784	9.41	134.77*

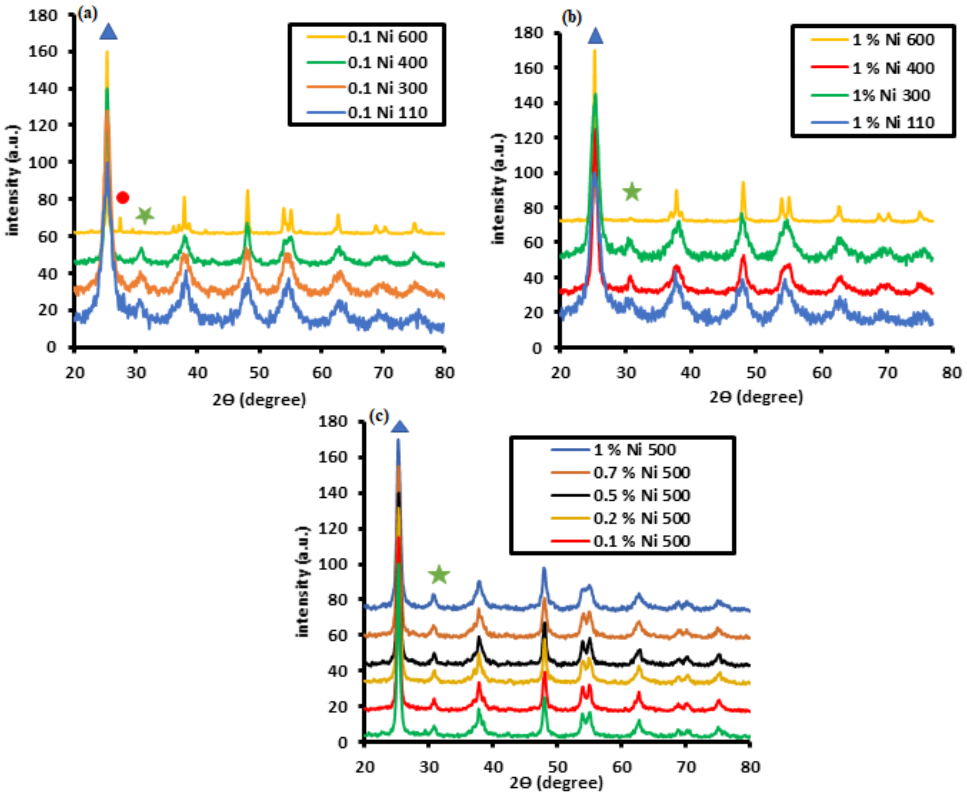

Fig. 3. XRD patterns of Ni-doped TiO_2 prepared with 10 mL ethanol and heated at different temperatures. (▲ Anatase phase, ● Rutile Phase, ★ brookite phase)

the mixture of anatase and brookite phases and the transition of anatase phase to rutile phase which started at 600 °C. It was reported that the use of acetic acid yields a pure and stable anatase phase at high temperatures (transition to rutile started at 750 °C). Also, some papers mentioned that transition occurred at higher temperatures (750–900 °C) [18, 30] and depend on the used precursor and the synthesis parameters [33]. The mean crystal dimension of TiO_2 was obtained by the Scherrer equation (Eq. 2) is shown in Fig. 2b. The obtained results showed that the mean size of the TiO_2 crystal was not depended on the ethanol volume but was dependent on the calcination temperatures. The lattice parameters of the samples were obtained according to Eq. 3 and therefore showed a tetragonal system. A little increase in volume cell was observed for the samples that were calcined at 500 °C (Table 3) and later on it decreased at 600 °C due to the rutile phase formation. The obtained unit cell parameters (Table 3) were in very good agreement with the results that reported elsewhere [40, 41]

The diffraction for the rutile phase was not observed in the XRD patterns of 0.5 and 1.0 % Ni-TiO_2 samples calcined at 600 °C whereas 0.1 % Ni 600 contained a little percentage of rutile phase (Fig. 3a and b). These results confirm that the addition of Ni(II) during the preparation of TiO_2 suppressed the formation of the rutile phase. This observation could be due to the replacement of Ti(IV) by Ni(II) in TiO_2 lattice. This result is the following that found in ref. [42]. Also, the addition of Ni(II) did not affect the percentage of brookite

Table 4. Mean crystal dimension of TiO_2 in Ni-doped samples.

Sample	0% Ni	0.1% Ni	0.2% Ni	0.5% Ni	0.7% Ni	1.0% Ni
Crystal Size of TiO_2 (nm)	16.39	17.46	16.06	15.75	14.60	12.75

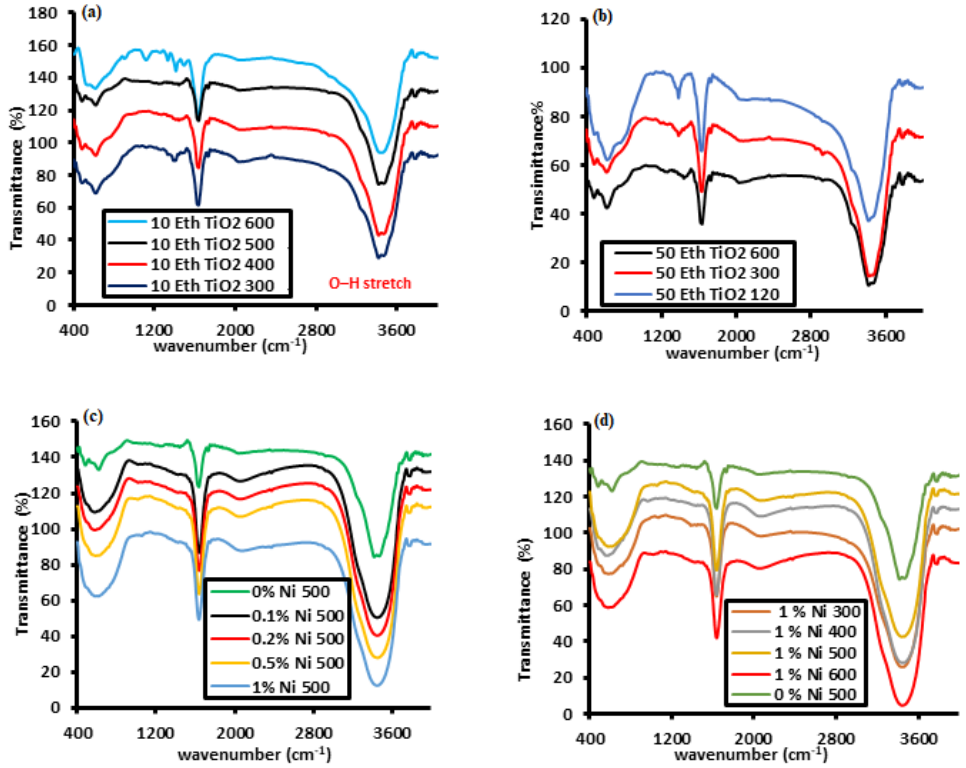

Fig. 4. FTIR spectra of TiO_2 prepared with (a) 10 mL, (b) 50 mL ethanol and heated at different temperatures; (c) different percentages of nickel and heated at 500 °C; (d) 1.0% of nickel and heated at different temperatures

phase at 500 °C (Fig. 3c).

Also, the mean crystal dimension of TiO_2 was calculated by the Scherrer equation for Ni-doped TiO_2 samples that were calcined at 500°C (Table 4). The dimension of TiO_2 crystal in Ni-doped samples (except 0.1% Ni) (Table 4) is smaller than pure TiO_2 (Fig. 2b). The Ni (II) radius (0.72 Å) is more than Ti(IV) (0.605 Å) and the nickel doping delayed the crystal growing of TiO_2 [35, 43]

FTIR spectroscopy

The vibrations at 3420 and 1620 cm^{-1} indicate hydroxyl groups of moisture existent on the surface of TiO_2 that are necessary for the generation of hydroxyl radicals during the photocatalytic degradation process (Fig. 4)[18]. The vibrations at 476 and 620 cm^{-1} are known as a fingerprint for Ti–O and Ti–O–Ti bonds [42]. The vibration shape and band frequency at 500 cm^{-1} (stretching vibration of Ti–O–Ti and Ti–O) in the FTIR spectra of the doped samples are different compared to pure TiO_2 (Fig. 4d). These observations could prove the structural rearrangement of the Ti–O–Ti environment after doping nickel that leads to the stressed network and alteration of the local symmetry [44]. There is no vibration of Ni-O (400-500 cm^{-1}) in the FTIR spectra of the doped samples due to the low amount of nickel which is not in the sensitivity range of FTIR analysis

The color change of TiO_2 was observed after nickel doping from white (pure TiO_2) to pale-yellow (Ni/TiO_2) samples. This yellow color remained unchanged after calcination up to 600 °C and proved nickel doping to TiO_2 lattice (Fig. 5).

Raman Spectroscopy

We applied Raman spectroscopy analysis for the identification of different phases of TiO_2. We detected anatase phase peaks for TiO_2 samples at 396, 514, and 636 cm^{-1} [18] and brookite phase

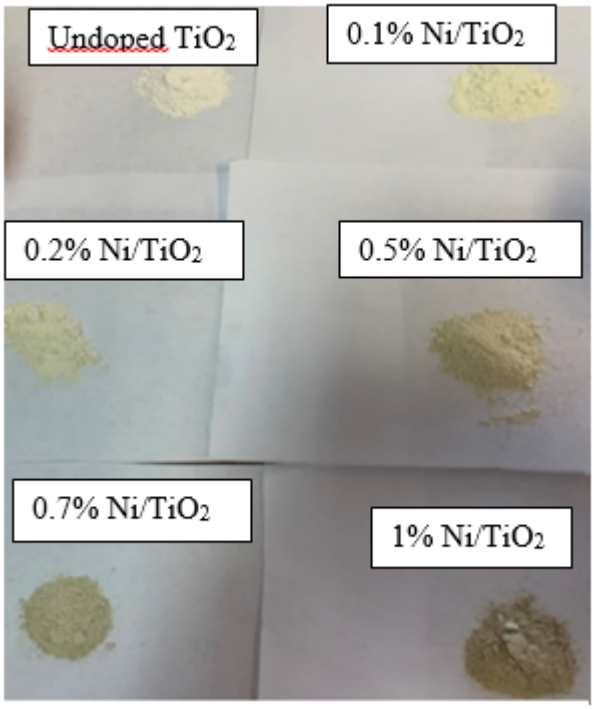

Fig. 5. The color of Ni-TiO_2 samples after treated at 500 °C.

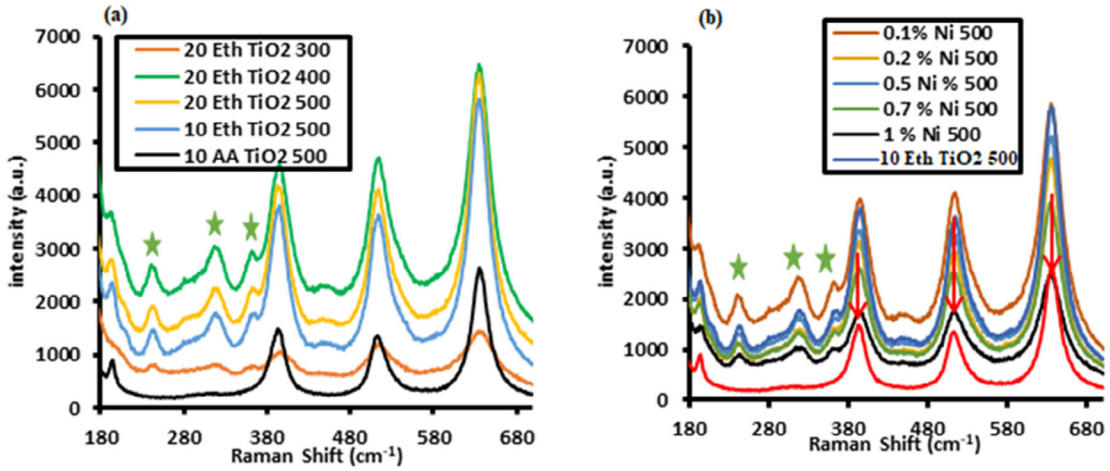

Fig. 6. Raman spectra of (a) TiO_2 samples prepared in the presence of 10 mL ethanol and (b) Ni-TiO_2 samples prepared in the presence of 10 mL ethanol heated at 500 °C (brookite phase*)

(several peaks in the zone 210 - 330 cm^{-1}) (Fig. 6) [36]. The Raman spectra of all the undoped and Ni-TiO_2 samples treated at a temperature below 600 °C indicated the presence of anatase and brookite phases.

SEM/ EDX analysis

The SEM images and EDX patterns of some samples are displayed in Figs. 7 to 9. The EDX patterns of pure TiO_2 indicated several strong peaks at different positions which correspond to oxygen and titanium (Fig. 7). The EDX analysis approves the attendance of nickel in the prepared samples (Fig.9 and Table 5). The peak for nickel in the EDX pattern of 0.2% Ni 500 sample was not observed due to the low amount of nickel, which is not in the sensitivity range of EDX analysis. Fig.s.7 and 8 display SEM images of undoped samples

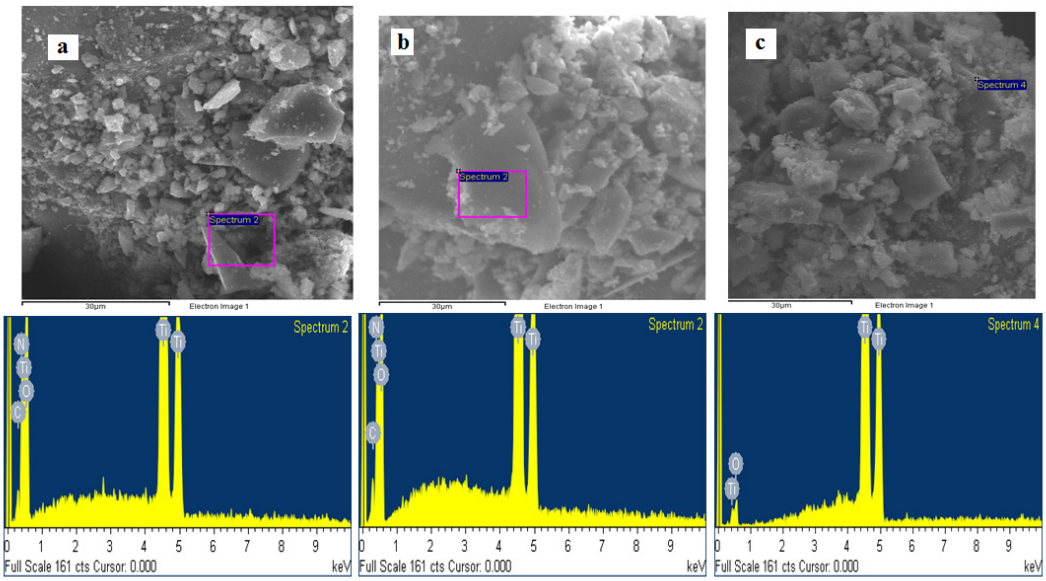

Fig. 7. SEM images and EDX patterns of a) 20 Eth 300, b) 20 Eth 400 and c) 20 Eth 500

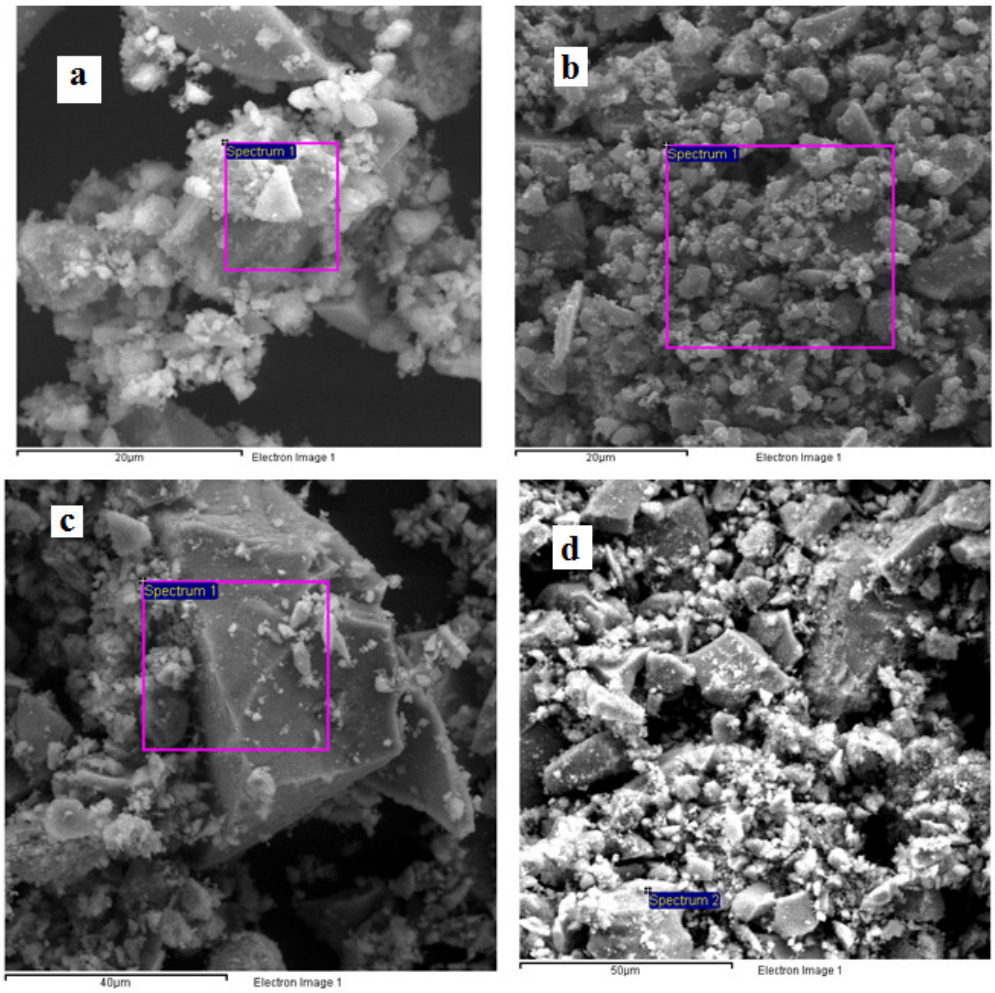

Fig. 8. SEM images of a) 0.2% Ni 500, b) 0.5% Ni 500 c) 0.7% Ni 500 and d) 1.0% Ni500

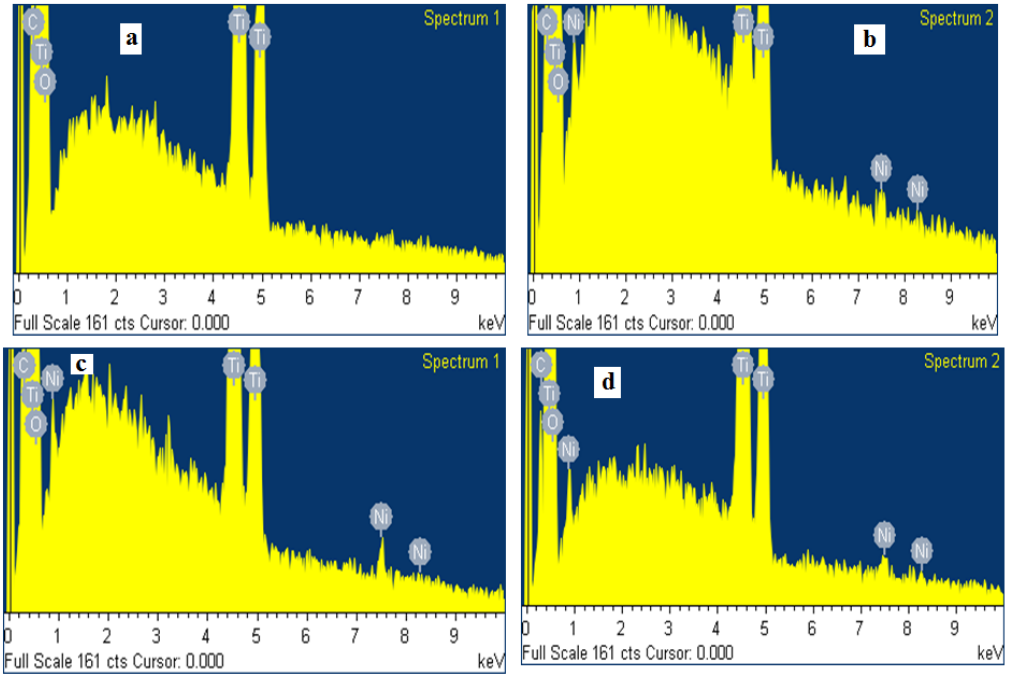

Fig. 9. EDX patterns of a) 0.2% Ni 500, b) 0.5% Ni 500 c) 0.7% Ni 500 and d) 1.0% Ni500

Table 5. EDX analysis of Ni-doped TiO_2 samples heated at 500 °C (At%: atomic %)

Sample	C (At%)	O (At%)	Ti (At%)	Ni (At%)
0.0% Ni 500	5.54	59.90	34.65	-
0.2% Ni 500	9.58	64.92	52.51	-
0.5% Ni 500	4.75	60.30	34.61	0.34
0.7% Ni 500	4.50	69.14	26.07	0.28
1.0% Ni 500	1.63	59.11	38.86	0.40

prepared with 20 mL ethanol and calcined at different temperatures and Ni-doped TiO_2 samples heated at 500 °C. The particles of all the samples have the same morphology (irregular shapes) and large aggregates.

Kinetic study

Effect of water in TiO_2 preparation

The variation of the UV- Visible spectrum of the dye versus time showed a decrease in the absorption with time (especially at λ_{max}) and confirmed degradation of the dye. Also, there was a shift in λ_{max} with time in the visible region that could be attributed to the successive elimination of amino and hydroxyl groups in the dye. The degradation efficiency of 10 Eth TiO_2 500 increased from 50.83 % to 89.22% by increasing the irradiation time from 16 min to 45 min. The degradation efficiency was determined through the following equation (5).

$$\text{Degradation efficiency (D\%)} = \frac{A_o - A_t}{A_o} \times 100 \quad (5)$$

Where A_o and A_t represent the initial absorbance and absorbance at any time t of E131 VF, respectively. The photocatalytic removal of E131 VF dye followed perfectly the first-order kinetics in the existence of TiO_2 (k_n: pseudo n order). The results of kinetic studies also showed that calcined samples at 500 ° C showed the best performance for the degradation of E131 VF dye (Fig. 10).

The results in Fig. 11a demonstrated that all the samples (except 50 Eth 600) with a high percentage of anatase phase showed good degradation performance of E131 VF dye due to the appropriate proportion in the mixture of two phases (anatase and rutile), lower energy of bandgap and synergistic effect of different phases in the degradation process [44].

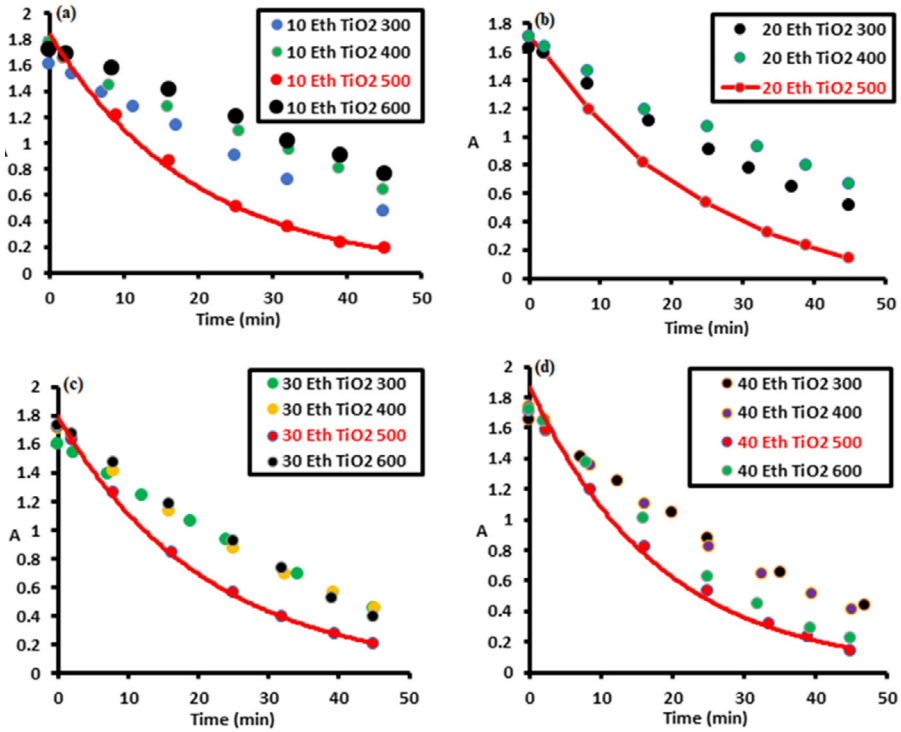

Fig. 10. Photocatalytic degradation of E 131 VF dye in the presence of TiO_2 prepared with different volumes of ethanol and calcined at different temperatures (a) 10 mL; (b) 20 mL; (c) 30 mL; (d) 40 mL ethanol

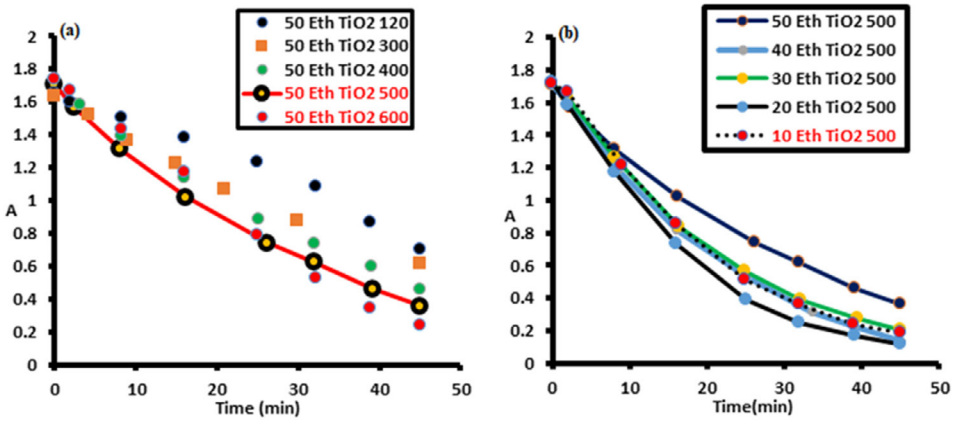

Fig. 11. Photocatalytic degradation of E 131 VF dye in the presence of (a) TiO_2 prepared with 50 mL ethanol and calcined at different temperatures; (b) TiO_2 prepared with different volumes of ethanol and calcined at 500 °C

In our previous work, we obtained pure anatase phase by the sol-gel procedure using acetic acid as an organic solvent and the highest crystallinity and performance were achieved in the presence of 10 mL acetic acid and calcination temperature at 500 °C [18]. According to the kinetic studies, TiO_2 samples that were prepared in the presence of acetic acid displayed higher catalytic activity (k_1= 0.083 (a.u.)) than the samples prepared in the presence of ethanol (k_1= 0.051 (a.u.)). So, it could be concluded that acetic acid is a better solvent to synthesize TiO_2 nanoparticles versus ethanol. The best rate constants k_1 (a.u.): 0.051 and 0.061 (Table 6) and high degradation efficiency 89.22% and 93.25% were obtained for the samples that were prepared using 10 and 20 mL ethanol and calcined

Table 6. Rate constant of the photocatalytic reaction obtained Ni-doped samples calcined at 500°C

Volume of ethanol (mL)	10	20	30	40	50
k_1 (a.u.)	0.051	0.061	0.048	0.035	0.034

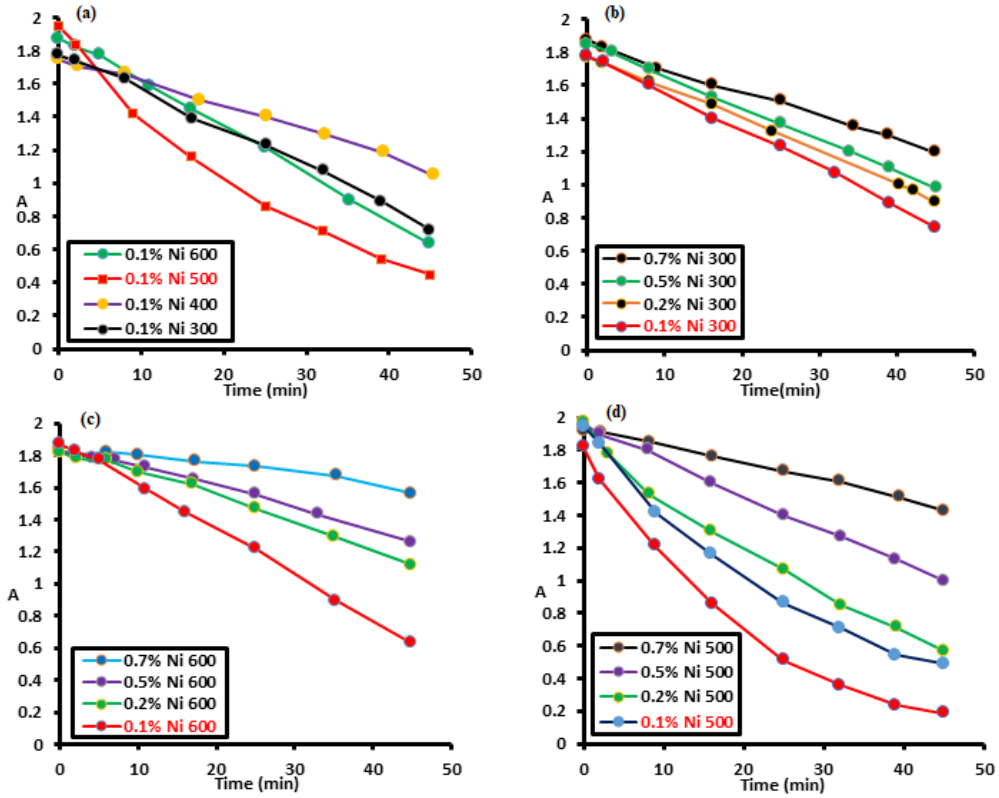

Fig. 12. Photocatalytic degradation of E131 VF in presence of Nickel doped TiO_2 and calcined different at temperatures

at 500 °C respectively. According to the above-mentioned results, we prepared Ni-doped samples in the presence of 10 mL ethanol and calcined them at different temperatures in order to achieve the best performance in the dye degradation. Ni-doped samples (except 0.1% Ni 500 where the order was 1) displayed zero-order kinetics for degradation of E131 VF dye. Similar results were obtained with Fe(II) doped titanium dioxide [45, 46].

A decrease in the photocatalytic efficiency was observed by increasing the Ni/TiO_2 ratio in all of the calcination temperatures (Fig. 12) and the best performance was achieved for 0.1% Ni 500 sample with the highest anatase phase (Fig. 12a). Also, a decrease in the rate constant was observed from 0.051 (a.u.) to 0.002 (a.u.) for 0% Ni 500 and 1% Ni 500 samples, respectively. Similar results were obtained in our previous work for Cu doped samples [4, 18]. Ni-doped samples showed lower photocatalytic activity compared to pure TiO_2 under UV irradiation that it could be attributed to the thickness of the doped atom layer and its screening effect.

The addition of water is necessary to accelerate the sol-gel process and gel formation. The kinetic study showed that the use of water is essential in the synthesis of titanium dioxide, as it results in the improvement of photocatalytic activity. Since the rate constant (k_1= 0.051 (a.u.)) of 10 Eth TiO_2 500 was synthesized in the presence of 100 mL H_2O is higher than the sample was prepared with 0.5 mL H_2O (k_1= 0.029 (a.u.)). It was reported that the increase in the molar ratio of water significantly increases the values of the bandgap energy, the specific surface area, and the anatase crystal phase [47]. However, the excessive water in the preparation results in the phase transition from anatase to rutile, as well as an increase in the crystal

Table 7. Band gap energy of Ni-doped samples heated at 500°C.

% Ni	0.0	0.1	0.2	0.5	0.7	1.0
Band gap energy (eV)	3.10	3.20	3.12	2.95	2.80	2.40

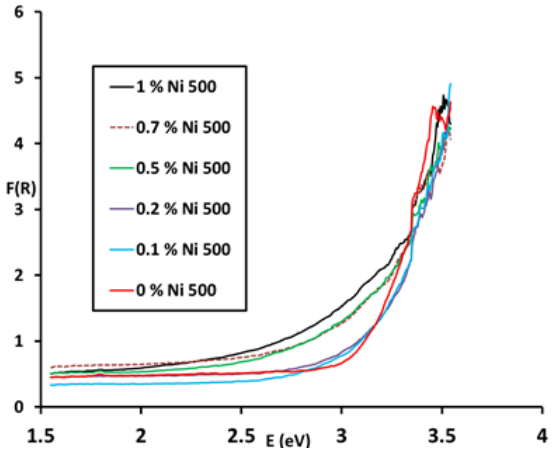

Fig. 13. Determination of bandgap energy of nickel doped TiO_2 calcined at 500 °C

size; thus, lowering the photocatalytic activity of TiO_2 [47, 48]. The anatase to rutile phase transition (ART) was influenced by hydrolysis rate through varying H_2O/Ti^{4+} ratio in the reaction system. Higher the water content, larger rutile particles will be formed after the thermal treatment and vice versa. In other words, increasing water content enhances the hydrolysis rate and the formation of larger particles thermodynamically favored anatase to the rutile phase transition. The important significance is that gelation time is effectively reduced by increasing the water concentration as it accelerates the cross-linking process [39].

It was reported that nickel was doped homogeneously in the form of Ni^{2+} into the crystal lattice of TiO_2, where it narrowed the bandgap and enhanced the absorption of visible light [49]. In our case, UV- Visible DR spectra showed that the bandgap energy decreased with the increase in Ni percentage but without shift of its optical response to the visible light range (Table 7, Fig. 13). It could be attributed to the formation of a new energy level intermediate between the valence and the conduction band of TiO_2. This new band traps the excited electron and prevents them from reaching the conduction band of TiO_2. Thus, it inhibits the formation of active radicals that are responsible for the degradation of the dye molecules. Also, many researchers attributed this decrease in degradation performance to several factors:

1. The increase in the recombination of electrons and holes is a function of the number of doping atoms that act as new trap electron centers [50].
2. The presence of an oxide layer at the surface of TiO_2 (screening effect)[31].
3. The lower crystallinity and transition of anatase phase into rutile phase in doped samples [51].
4. The agglomeration of TiO_2 nanoparticles during solvation, so the particles are not well dispersed in the solution of pollutants. Thus, the surface area available for photon absorption would be reduced[45].
5. Trapping of the electrons by doped metals, thus inhibiting the formation of active radicles responsible for the degradation of pollutant molecules [18].
6. The photoactivity is declined when the amount of the doping metal exceeds some percentage [52].

Among these factors, the decrease in the photoactivity in our case is probably a result of electrons trapping by nickel, agglomeration of TiO_2 nanoparticles, and the amount of Ni(II) doped.

Effect of radiation wavelength

It is well known that the bandgap energy of TiO_2 is around 3.2 eV and active under UV irradiation. Several researchers reported that doping TiO_2 with metal leads to a shift in its optical response toward the visible light region (redshift)[31]. For

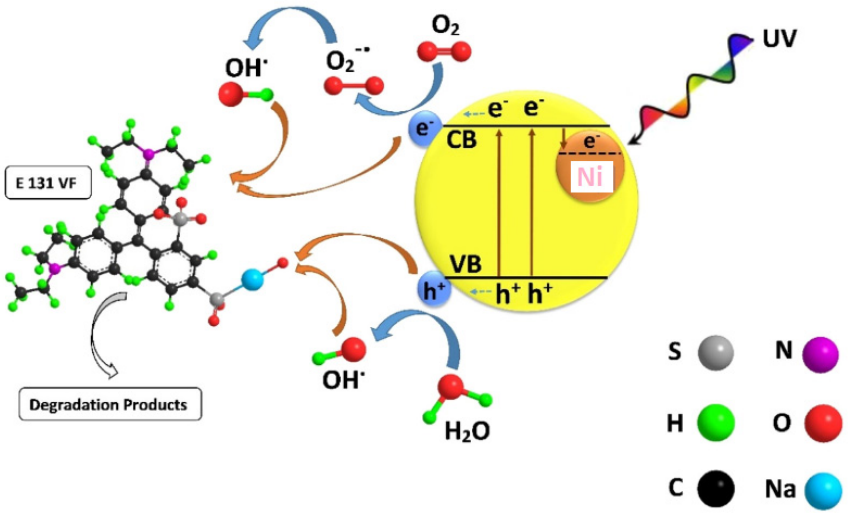

Fig. 14. Proposed mechanism for photocatalytic degradation of E 131 VF dye by Ni-doped TiO_2 sample under UV irradiation.

this reason, the photocatalytic activity of 0.5% Ni 500 was tested at several λ (256, 320, 360 nm, and visible (white lamp)) to detect the maximum wavelength for the best catalytic activity. According to this study, the photocatalytic activity of TiO_2 remained approximately constant at 256, 320, 360 nm, and under visible light, no degradation occurs. We have two possibilities here. Either there is an insertion of nickel inside TiO_2 crystal lattice, where it decreases the bandgap energy and forms defect sites resulting in the recombination of electrons and holes [49], or nickel atoms don't enter into TiO_2 crystal lattice and therefore are dispersed onto the TiO_2 surface (screening effect), where it reduces the quantity of radiation reaching to the photocatalyst. More investigations are needed to understand the main reason for it.

Proposed mechanism for E 131 VF dye degradation

Our proposed mechanism for photocatalytic degradation of E 131 VF dye is shown in Fig. 14. High-energy electrons are produced on Ni-doped TiO_2 surfaces under UV irradiation. These electrons are transferred from the valance band to the conduction band of TiO_2 and the holes remain on the valance band of TiO_2. The oxygen molecules adsorbed on the surface of photocatalyst trap the electron from TiO_2 and thus several active species including $OH^{\cdot}$ and $O_2^{\cdot -}$ radicals are formed. These active species attack E 131 VF dye molecules and degrade them. The photoinduced holes (h^+) could react with H_2O molecules and oxidize them to $OH^{\cdot}$ radicals or oxidize the dye molecules. Also, the results of E 131 VF photocatalytic degradation (Figs. 11 and 12) revealed that degradation rates in the presence of nickel-doped TiO_2 samples were lower than pure TiO_2 under UV irradiation. The recombination of photoinduced charge carriers is one of the most main factors that decline the photocatalytic performance of TiO_2 samples. Therefore, any factor that overcomes the recombination of charge carriers will improve photoactivity. In Ni-doped samples, nickel ions may act as recombination sites or trap the electrons from the TiO_2 conduction band, hence decrease the photoactivity. It is reported that the optimal concentration of doping ions should create the thickness of the space charge layer considerably equal to the light penetration depth [29]. In the author's point of view, further studies are required for the study of several parameters such as (1) TiO_2 synthesis method and doping procedure for reducing the aggregation of TiO_2 nanoparticles, (2) the concentration of nickel ion for controlling the thickness of space charge layer and (3) the nature of solvents and their quantities for controlling the morphology and phase structure of TiO_2 nanoparticles to improve the performance of Ni-doped TiO_2 samples compared to pure TiO_2.

CONCLUSIONS

In this work, TiO_2 nanoparticles were prepared by a sol-gel procedure using ethanol as solvent. The best crystallinity was achieved for the samples that were calcined at 500 °C. The XRD results showed that the transition of the anatase phase to the rutile

phase was related to the volume of ethanol and calcination temperature. Also, XRD data displayed that the fraction of the anatase phase increased by increasing ethanol volume. The addition of Ni(II) suppressed the formation of the rutile phase. The mean crystal size of TiO_2 increased by the rising of calcination temperature. The best photocatalytic performance was obtained for the samples prepared in the presence of 10 or 20 mL ethanol and annealed at 500 °C. These conditions were applied for the preparation of nickel-doped samples. The synergetic effect is observed between anatase and rutile phases at 600 °C. A negative effect on the photoactivity of TiO_2 has been observed with an increase in Ni (II) amount, because of the formation of a new energy level intermediate between the valence and conduction bands of TiO_2 (trapping centers). Thus, inhibiting the formation of active radicals that are responsible for the degradation of the dye molecules.

ACKNOWLEDGMENT

The author thanks Prof. Michel Kazan to help us doing some analyses at the American University of Beirut and also the Lebanese University for providing financial assistance to carry out this work.

DISCLOSURE STATEMENT

No potential conflict of interest was reported by the authors.

REFERENCES

1. Chen B, Wang M, Duan M, Ma X, Hong J, Xie F, et al. In search of key: Protecting human health and the ecosystem from water pollution in China. Journal of Cleaner Production. 2019;228:101-11.
2 Wankhade AV, Gaikwad GS, Dhonde MG, Khaty NT, and Thakare SR. Removal of Organic Pollutant from Water by Heterogenous Photocatalysis: A Review. Res. J. Chem. Environ. 2013;17(1):84–94.
3. Lin W-S, He PH, Chau C-F, Liou B-K, Li S, Pan M-H. The feasibility study of natural pigments as food colorants and seasonings pigments safety on dried tofu coloring. Food Science and Human Wellness. 2018;7(3):220-8.
4 El Tfayli F, Makki M, Kassir M, El Jamal M, and Pirbazari AE. Photocatalytic Removal of Food Colorant E 131 VF from synthetic wastewater by Cu Doped TiO_2 Samples. **J.Wat.Env.Nanotech.** 2019;4(3):187–197.
5. Mallah HA, Naoufal DM, Safa AI, El-Jamal MM. Study of the Discoloration Rate of Rhodamine B as a Function of the Operating Parameters at Pt and BDD Electrodes. Portugaliae Electrochimica Acta. 2013;31(3):185-93.
6 El Jamal MM and Ncibi MC. Biosorption of methylene blue by chaetophora elegans algae: Kinetics, equilibrium and thermodynamic studies. Acta Chim. Slov. 2012;59(1): 24–31.
7. Naser Elddine HA, Damaj ZK, Yazbeck OA, Tabbara MA, El-Jamal MM. Kinetic Study of the Discoloration of the Food Colorant E131 by K2S2O8 and KIO3. Portugaliae Electrochimica Acta. 2015;33(5):275-88.
8 Selivanovskaya S, Kuryntseva P, and Galitskaya P. Eco-Toxicity Dynamics in Compost Prepared From Organic Wastes. September - October, Res. J. Pharm. , Biol. Chem. Sci. 2015;6(5):1606–1610.
9. Ghasemi B, Anvaripour B, Jorfi S, Jaafarzadeh N. Enhanced Photocatalytic Degradation and Mineralization of Furfural Using UVC/TiO2/GAC Composite in Aqueous Solution. International Journal of Photoenergy. 2016;2016:1-10.
10. Noman MT, Ashraf MA, Ali A. Synthesis and applications of nano-TiO2: a review. Environmental Science and Pollution Research. 2018;26(4):3262-91.
11. Lee KM, Lai CW, Ngai KS, Juan JC. Recent developments of zinc oxide based photocatalyst in water treatment technology: A review. Water Research. 2016;88:428-48.
12. S S, E T, M K, B G, M Y. Compared with a-Fe2O3 and ZnxFe3-XO4 Thin Films Grown by Chemical Spray Pyrolysis. International Journal of Sensor Networks and Data Communications. 2017;06(01).
13. Riazian M, Yousefpoor M. Photocatalytic activity, nanostructure and optical properties of 3D ZnS urchin-like via hydrothermal method. International Journal of Smart and Nano Materials. 2020;11(1):47-64.
14. Ullattil SG, Periyat P. Sol-Gel Synthesis of Titanium Dioxide. Advances in Sol-Gel Derived Materials and Technologies: Springer International Publishing; 2017. p. 271-83.
15. Pigeot-Rémy S, Gregori D, Hazime R, Hérissan A, Guillard C, Ferronato C, et al. Size and shape effect on the photocatalytic efficiency of TiO2 brookite. Journal of Materials Science. 2018;54(2):1213-25.
16. Gardon M, Guilemany JM. Milestones in Functional Titanium Dioxide Thermal Spray Coatings: A Review. Journal of Thermal Spray Technology. 2014;23(4):577-95.
17. Wei X, Zhu G, Fang J, Chen J. Synthesis, Characterization, and Photocatalysis of Well-Dispersible Phase-Pure Anatase TiO2Nanoparticles. International Journal of Photoenergy. 2013;2013:1-6.
18. Ali Makki F, Hassan MAEH, El Jamal MM, Tabatabai-Yazdi F-S, Ebrahimian Pirbazari A. Kinetic evaluation of photocatalytic degradation of food colorant E 131 VF by copper doped TiO2 nanophotocatalysts prepared at different calcination temperatures. Environmental Technology & Innovation. 2020;19:100981.
19. Qian R, Zong H, Schneider J, Zhou G, Zhao T, Li Y, et al. Charge carrier trapping, recombination and transfer during TiO2 photocatalysis: An overview. Catalysis Today. 2019;335:78-90.
20. Bamne J, Taiwade K, Sharma PK, Haque FZ. Effect of calcination temperature on the growth of TiO2 nanoparticle prepared via sol-gel method using triton X-100 as

surfactant. Author(s); 2018.
21. Nguyen VN, Nguyen NKT, Nguyen PH. Hydrothermal synthesis of Fe-doped TiO 2 nanostructure photocatalyst. Advances in Natural Sciences: Nanoscience and Nanotechnology. 2011;2(3):035014.
22. Ramakrishnan VM, Natarajan M, Santhanam A, Asokan V, Velauthapillai D. Size controlled synthesis of TiO 2 nanoparticles by modified solvothermal method towards effective photo catalytic and photovoltaic applications. Materials Research Bulletin. 2018;97:351-60.
23. Kumar A. Different Methods Used for the Synthesis of TiO2 Based Nanomaterials: A Review. American Journal of Nano Research and Applications. 2018;6(1):1.
24 Kožáková Z, Mrlík M, Sedlačík M, Pavlínek V, and Kuřitka I. Preparation of TiO_2 powder by microwave-assisted molten-salt synthesis. NanoCON. 2011;9:2–7.
25. Kathirvel S, Su C, Shiao Y-J, Lin Y-F, Chen B-R, Li W-R. Solvothermal synthesis of TiO2 nanorods to enhance photovoltaic performance of dye-sensitized solar cells. Solar Energy. 2016;132:310-20.
26. Siddiqui H. Modification of Physical and Chemical Properties of Titanium Dioxide (TiO2) by Ion Implantation for Dye Sensitized Solar Cells. Ion Beam Techniques and Applications: IntechOpen; 2020.
27. Zulfiqar M, Chowdhury S, Samsudin MFR, Siyal AA, Omar AA, Ahmad T, et al. Effect of organic solvents on the growth of TiO2 nanotubes: An insight into photocatalytic degradation and adsorption studies. Journal of Water Process Engineering. 2020;37:101491.
28. Di Paola A, García-López E, Ikeda S, Marcì G, Ohtani B, Palmisano L. Photocatalytic degradation of organic compounds in aqueous systems by transition metal doped polycrystalline TiO2. Catalysis Today. 2002;75(1-4):87-93.
29. Pirbazari AE, Monazzam P, Kisomi BF. Co/TiO2 nanoparticles: preparation, characterization and its application for photocatalytic degradation of methylene blue. DESALINATION AND WATER TREATMENT. 2017:283-92.
30. Lin Y-M, Jiang Z-Y, Zhu C-Y, Hu X-Y, Zhang X-D, Fan J. Visible-light photocatalytic activity of Ni-doped TiO2 from ab initio calculations. Materials Chemistry and Physics. 2012;133(2-3):746-50.
31. Ganesh I, Gupta AK, Kumar PP, Sekhar PSC, Radha K, Padmanabham G, et al. Preparation and Characterization of Ni-Doped Materials for Photocurrent and Photocatalytic Applications. The Scientific World Journal. 2012;2012:1-16.
32. Alosfur FKM, Ouda AA, Ridha NJ, Abud SH. High photocatalytic activity of TiO2 nanorods prepared by simple method. Materials Research Express. 2019;6(6):065028.
33. Bakri AS, Sahdan MZ, Adriyanto F, Raship NA, Said NDM, Abdullah SA, et al. Effect of annealing temperature of titanium dioxide thin films on structural and electrical properties. Author(s); 2017.
34. Mahyar A, Amani-Ghadim AR. Influence of solvent type on the characteristics and photocatalytic activity of TiO2 nanoparticles prepared by the sol–gel method. Micro & Nano Letters. 2011;6(4):244.
35. Monazzam P, Ebrahimian Pirbazari A, Khodaee Z. Enhancement of visible light photoactivity of rutile-type TiO2 by deposition of silver onto Co-TiO2/MWCNTs nanocomposite for degradation of 2,4-dichlorophenol. Materials Chemistry and Physics. 2019;228:263-71.
36. Chalastara K, Guo F, Elouatik S, Demopoulos GP. Tunable Composition Aqueous-Synthesized Mixed-Phase TiO2 Nanocrystals for Photo-Assisted Water Decontamination: Comparison of Anatase, Brookite and Rutile Photocatalysts. Catalysts. 2020;10(4):407.
37. Phromma S, Wutikhun T, Kasamechonchung P, Eksangsri T, Sapcharoenkun C. Effect of Calcination Temperature on Photocatalytic Activity of Synthesized TiO2 Nanoparticles via Wet Ball Milling Sol-Gel Method. Applied Sciences. 2020;10(3):993.
38. Kandiel TA, Robben L, Alkaim A, Bahnemann D. Brookite versus anatase TiO2photocatalysts: phase transformations and photocatalytic activities. Photochem Photobiol Sci. 2013;12(4):602-9.
39. Kumar SG, Rao KSRK. Polymorphic phase transition among the titania crystal structures using a solution-based approach: from precursor chemistry to nucleation process. Nanoscale. 2014;6(20):11574-632.
40. Ghasemi S, Rahimnejad S, Setayesh SR, Rohani S, Gholami MR. Transition metal ions effect on the properties and photocatalytic activity of nanocrystalline TiO2 prepared in an ionic liquid. Journal of Hazardous Materials. 2009;172(2-3):1573-8.
41. Madhusudan Reddy K, Gopal Reddy CV, Manorama SV. Preparation, Characterization, and Spectral Studies on Nanocrystalline Anatase TiO2. Journal of Solid State Chemistry. 2001;158(2):180-6.
42. Singla P, Pandey OP, Singh K. Study of photocatalytic degradation of environmentally harmful phthalate esters using Ni-doped TiO2 nanoparticles. International Journal of Environmental Science and Technology. 2015;13(3):849-56.
43. Pal M, Pal U, Jiménez JMGY, Pérez-Rodríguez F. Effects of crystallization and dopant concentration on the emission behavior of TiO2:Eu nanophosphors. Nanoscale Research Letters. 2012;7(1).
44. Mushtaq K, Saeed M, Gul W, Munir M, Firdous A, Yousaf T, et al. Synthesis and characterization of TiO2 via sol-gel method for efficient photocatalytic degradation of antibiotic ofloxacin. Inorganic and Nano-Metal Chemistry. 2020;50(7):580-6.
45 Estephane GC, and El Jamal MM. Effect of doping of TiO_2 nanoparticles with silver on their photocatalytic activities toward degradation of E 131 VF. J. Chem. Technol. Metall., 2019;54(5):926–933.
46. Estephane GC, Kassir MM, El Jamal MM. Kinetic Study of the Metal Ions Doped TiO2 Samples for the Photocatalytic Degradation of E 131 VF. Portugaliae Electrochimica Acta. 2020;38(6):365-76.
47. May-Lozano M, Ramos-Reyes GM, López-Medina R, Martínez-Delgadillo SA, Flores-Moreno J, Hernández-Pérez I. Effect of the Amount of Water in the Synthesis of

B-TiO2: Orange II Photodegradation. International Journal of Photochemistry. 2014;2014:1-8.

48. Xie L, Li Z, Sun L, Dong B, Fatima Q, Wang Z, et al. Corrigendum: Sol-gel Synthesis of TiO2 With p-Type Response to Hydrogen Gas at Elevated Temperature. Frontiers in Materials. 2019;6.
49. Gao B, Wang T, Fan X, Gong H, Guo H, Xia W, et al. Synthesis of yellow mesoporous Ni-doped TiO2 with enhanced photoelectrochemical performance under visible light. Inorganic Chemistry Frontiers. 2017;4(5):898-906.
50 Begum T, Gogoi PK, Bora U. Photocatalytic degradation of crystal violet on the surface of Au doped TiO_2 nanoparticles," Indian J. Chem. Technol., 2017;24:97–101,.
51 Taherinia M, Nasiri M, Abedini E, Pouretedal HR. The effect of solvent of titanium precursor in the sol-gel process on the activity of TiO_2 nanoparticles for H_2 production, Iranian Journal of Hydrogen & Fuel Cell, 2017;2:139–151.
52 Devi LG, Kottam N, Murthy BN, and Kumar SG. Journal of Molecular Catalysis A : Chemical Enhanced photocatalytic activity of transition metal ions Mn^{2+}, Ni^{2+} and Zn^{2+} doped polycrystalline titania for the degradation of Aniline Blue under UV / solar light, J. Mol. Catal. A, Chem. 2010;328(1–2):44–52.